A Simulation of the Attainment of High Potentials by the Use of Radium

R.A. Ryan

Christopher Newport University

Advisor: Dr. David Gore

Abstract

This project investigated the results and problems encountered by H.G.J. Moseley and John Harling Fellow in their 1913 experiment on attaining high potentials from a radioactive source (Moseley and Fellow 471-476). I designed and developed a computer simulation which models the apparatus they built in order to recreate their results by implementing the physical processes which governed their experiment. The simulation allows a user to easily interact with and manipulate the simulated apparatus. The problems Moseley and Fellow encountered appear to be due to the apparatus' inability to maintain a high potential without discharge due to arcing. Through the simulation, I was able to continue their work and investigate further into the attainment of high potentials created by the use of a radioactive isotope.

Background

In 1913, H.G.J. Moseley and John Harling Fellow published their attempts to decelerate the swiftest β-particles of a radioactive source. They did this by using the principle employed in Strutt's Radium Clock (Moseley and Fellow 471). Strutt's Radium Clock was an evacuated glass container with an inner cylinder containing a small amount of radium. As the radium decayed, it ejected β-particles. The β-particles collected on two foil leaves which, being similarly charged, repelled each other until they diverged enough to contact the silvered outer container walls. The outer walls were grounded to the inner cylinder, which allowed the charges to equalize once contact was made. This let the leaves

return to their original positions and begin the process again (Collins 266-267). Moseley and Fellow's apparatus was similar: The apparatus consisted of an evacuated flask (Figure 1.F) which held a small bulb containing radium (Figure 1.B) supported by a fine silica rod (Figure 1.R). The bulb contained radium emanation, commonly known as radon gas. Both the bulb and flask were silvered to be conductive. An aluminum disc was suspended inside the device by a silica spring which acted as an electrometer. By measuring the displacement of the disc, the force of attraction could be measured, which determined the voltage between the bulb and the outer flask (Moseley and Fellow 471-472).

Despite many attempts and many changes in the design of their apparatus, Moseley and Fellow were never able to achieve the voltages they anticipated. This was due to what they described as "accidents" wherein the inner bulb and outer surface would discharge by arc before any voltage higher than 150 kV could be achieved. At times, the arcing was violent enough to destroy the apparatus, which then had to be rebuilt. In their final attempt, they were able to achieve a stable voltage of around 110 kV. They accredited this to a slight current passing along the silica rod supporting the inner bulb. The current was attributed to less care having been taken in cleaning the rod during the building of the apparatus. They believed the current was just enough to keep the voltage below the arcing voltage and allowed equilibrium to be achieved. Their conclusion was that this was not a viable method of attaining high potentials due to the difficulties they encountered (Moseley and Fellow 474-476).

Purpose

Moseley and Fellow had difficulties controlling the variables in their experiment. This ultimately led to them abandoning the line of research. Better control of an experiment allows a researcher to manipulate one variable at a time to see how it affects the overall system. Any real world apparatus will introduce random and systematic errors. Modern computer simulations allow researchers to fully control an experiment. The validity of Moseley and Fellow's findings, as well as the viability of

their apparatus as a means to attain high potentials, can be investigated by creating a computer simulation of the experiment. Mathematical modeling of the physical phenomena which take place in the apparatus allows further experimentation to be done without being concerned with accidents, uncontrolled variables, and damaged equipment. By developing a simulation of their apparatus, it will be shown that the attainment of high potentials by the use of radium is possible and, furthermore, that the design of the apparatus governs the final potential obtained.

Process

A simulation of Moseley and Fellow's apparatus consists of implementing the mathematical equations governing the physical phenomena of the device in such a way that they produce a result which agrees with experimental values. These phenomena include: nuclear decay of an unstable isotope, acceleration of charged particles traversing an electrical potential, relativistic interactions of highly energetic particles, capacitance of the device, voltage of the device, electric field inside the device, and electron scattering of the particles of the outer flask. Research and investigation into these and other physical processes such as: β-particle emission from radon, traversal of the space between the inner bulb and outer flask, β-particle collection upon the outer surface, and after-effects on subsequent particles describe the main phenomena to be studied. The loss of energy of β-particles as they travel through: the gasses within the inner bulb, glass of the inner bulb, silvered surface, residual gas between the bulb and flask, and discharge due to gamma ray production of the source also need to be incorporated to build an accurate model.

An efficient model requires simplifying assumptions and an analysis of their impact on the accuracy of the model. In some cases, mathematical integration is not feasible due to complexity, and iterative solutions are implemented. Iterative solutions introduce error. A model becomes less accurate as the size of the iterative step increases.

Once an understanding of the processes involved is developed, implementation of the equations can be incorporated into the model and the simulation can be built. My simulation consists of individual classes representing parts of the model. A class is a construct which encapsulates the data and operations, which act upon the data, of an object. In this way, the program allows the individual classes to perform as independently as possible within the overall program. The user interface gives the user easy access to variables, results, and trials. A clock governs the steps of the program as it runs.

The main physical processes of the simulation are the decay of the isotope creating β-particles, the loss of energy as the β-particle travels up the potential, relativistic effects, and the potential difference developed by β-particles collecting upon the outer flask. I detail the implementation of these processes below.

Unstable Isotope Class

The decay of an isotope can produce a number of particles. For this simulation, the main particle of interest is the electron (or β-particle). The source used in the original Moseley and Fellow experiment was approximately 20 mCi of radon gas (Moseley and Fellow 472). Radon does not directly produce β-particles. Instead, radon decays by α-decay into polonium-218. This decays by α-decay into lead-214 which decays by β-decay into bismuth-214 (Firestone "*The Isotopes Project*"). Thus, the first instance of a β-particle being produced is three steps down the decay chain. The half-life (time it takes for one half of the atoms to decay) of bismuth-214 is only 20 minutes. Thus, bismuth-214 quickly decays by β-decay into polonium-214 which decays by α-decay into lead-210. While lead-210 is not stable (half-life of 22.3 years), for the duration of the simulation, lead-210 is considered to be a stable isotope. From the decay chain, it is seen that the majority of β-particles produced actually come from bismuth-214 and lead-210. Since the original experiment only mentions the initial amount of radon, it is assumed that the radon has decayed to the point of equilibrium with its daughter particles, which produced the β-particles.

A decay chain can reach an equilibrium of sorts if the daughter particles have shorter half-lives than the parent particles. The parent's decay rate effectively limits the amount of daughter available to decay, thus limiting the number of daughter decays to a rate similar to that of the parent. Within the decay chain of radon to lead-210, each daughter – with the exception of polonium-218 and lead-210 – has a shorter half-life than the parent. The consecutively shorter half-lives allow the particles to reach an equilibrium after a time.

To calculate the particles of each daughter, the simulation begins with the user-selected amount of isotope. This is the amount initially inside the inner bulb of the apparatus. Upon loading the simulation, the isotope must be aged to create the daughter particles which eject the β-particles. The simulation ages the isotope over 4 hours, which is sufficient to develop enough daughter particles in the chain to have stability in the simulation. To age the isotope, Equation U.3 (Appendix C) is used to calculate the number of parent and daughter atoms left at each time step for the four-hour aging time. The chosen time step is one second, which gives significant resolution to the calculations without creating dramatically long load times. The four-hour aging time is chosen to decay the source adequately enough to give a head start on the equalization process but not so long as to have depleted the source. Once aging has finished, the simulation can be run.

While the simulation runs, the number of each species in the decay chain is recursively calculated. This is done because, to know how many particles of a particular isotope there are to decay currently, it must be known how many decays the parent isotope had which create the isotope in question during the current time step. From this, the number of α-particles, β-particles, and γ-rays can be determined. The γ-rays are a product of some decay species and are incorporated into the simulation to determine the ejection of electrons from the outer flask, as discussed in the Capacitor Class section. The α-particles are counted and considered because their density builds within the inner bulb. Collisions with the α-particles decelerate electrons as they pass through the inner bulb also discussed in

the Capacitor Class section.

Equation U.1 (Appendix C) is used to give an energy distribution to the β-particles once they are counted. The equation was developed to mimic the energy distribution curves of β emitters. This adds accuracy to the model without adding further complication and focuses on developing a potential, rather than nuclear physics. Equation U.1 (Appendix C) is a skewed exponential curve which allows groupings of electrons to be assigned an energy value between zero and the maximum energy of the decay. The electrons are divided into energy groups by percentage of total electrons based on fitting the distribution curve. They are then further subdivided into random groups to give a more natural time distribution to the values. This keeps them true to the experimental energy distribution. These subgroups are assigned their energies and then returned as a collection of packets. By using packets of β-particles, rather than individual β-particles, the system requirements are reduced. The error is minimized by keeping the time steps small. As mentioned previously, increasing the time scale increases the error. Once the packets are assigned energies, the packets are then treated as individual β-particles until they reach the outer flask where they are counted in full by the capacitor class.

Capacitor and Electron Class

The capacitor is the representation of the physical apparatus of the simulation. The capacitor contains the radioactive source material. Once the source decays, it passes its β-particles (electrons) to the capacitor, which tracks and affects the electrons as they traverse from the inner bulb to the outer flask wall. The electrons undergo loss of energy both through interactions with matter such as glass, silver, and air; and through work climbing the potential.

The energy loss due to collisions with the gaseous materials inside the inner bulb is considered in the simulation. Equation C.4 (Appendix A) requires information on the scattering cross section of the materials interacting with the electron. The materials within the inner bulb are the radon gas and the

daughter particles the radon creates. Fortunately, the values for each of the daughter particles is very similar so, for the purpose of simplification, the values for radon alone are used. The α-particles, on the other hand, have a very different cross section and, are considered separately. Since α-particles can attract free electrons inside the inner bulb, they quickly become helium atoms. Therefore, the cross section data for helium is used. The number of α-particles increases over time due to the decay of radon and the daughter particles which decay by α-decay; thus, the effects upon the electrons increase over time. The effect on the electron from the other materials the electron passes through does not change over time. The glass of the inner bulb, the silver coating, and the residual gas inside the outer flask reduce the energy of the electron. These reductions are calculated in the simulation with Equation C.4 (Appendix A) .

In addition to energy loss from passing through materials, the electrons also pass through the electric field produced by the charged inner bulb. As electrons leave and collect on the outer flask, a positive charge equal to the number of electrons in flight plus those which have collected upon the outer flask wall collects on the inner bulb. The electrons lose energy as they climb the potential, according to Equations E.1 (Appendix B) and C.2 (Appendix A) . As the potential increases, more energy is needed by the electrons to make it the full distance to the outer flask wall. If the electrons do not make it the full distance, they are turned back and return to the inner bulb and do not add to the potential. In this way, the capacitor builds a voltage which limits the number of electrons able to contribute to the voltage over time, thus limiting the maximum voltage. The voltage of the capacitor increases as electrons collect on the outer flask. The voltage can be reduced by removing or dislodging electrons from the outer flask wall, allowing them to be drawn back to the inner bulb.

Some of the daughter particles of radon produce γ-rays. These γ-rays interact with the material of the outer flask and dislodge electrons by the photoelectric effect, which is represented by Equation C.4 (Appendix A). The positively charged inner bulb attracts the freed electrons and collects them,

reducing the positive charge on the inner bulb. Although small, the effect from the photon bombardment does make a noticeable difference. To simplify the simulation, all γ-rays are assigned an average energy of 1 MeV rather than trying to fit values to a curve. The averaging of the energy does not have a dramatic affect on the discharge.

Results

By making some assumptions on the exact construction of Moseley and Fellow's apparatus, the simulation successfully models their device. The values the model produces are realistic and allow easy manipulation of the variables of the experiment. The simulation suggests that by producing a vacuum of less than 12 mTorr inside a one liter silvered flask with a smooth silvered inner bulb containing 20 mCi of radon gas in equilibrium with shorter-lived daughter particles, it is possible to achieve an electric potential great enough to turn back the most energetic β-particles which escape the inner bulb.

Discussion

As Moseley and Fellow discovered, even in a high vacuum, discharge by arcing is possible. Paschen's Law describes breakdown voltage and can model the arcing effect (Wadwha 13). The dependent variable of the curve described by Paschen's Law is the product of pressure and distance. The law accurately models arcing between two charged surfaces for high pressure-distance values, but other factors begin to govern the arcing effect as the pressure-distance value decreases. Moseley and Fellow state that their earlier apparatus would charge to between 100-150 kV before arcing.

Equation S.1 (Appendix D) gives the breakdown voltage between two electrodes in a uniform electric field. The constants for air have been experimentally found for, A, B, and v, as 12 $s^2 kg^{-1}$, 365 $cm^2 s^{-1} A^{-1,}$ and 0.02, respectively (Wadhwa 13). Moseley and Fellow claimed they were able to sustain a voltage of 110 kV in their final apparatus. Using this voltage and Equation S.1 (Appendix D),

we can infer that the vacuum they attained was at least 12.04 mTorr. Should they have had a vacuum more than 12.04 mTorr, their apparatus would have arced below 110 kV assuming a perfectly smooth surface. A theory on arcing in high vacuum suggests that, at low pressure distance values, sharp points on a rough surface collect enough charge to be pulled free from the electrode. Once free, the charged particles gain enough energy over the distance traveled to ionize the opposing electrode and free oppositely charged particles. These particles gain energy crossing the distance in the opposing direction. This causes a rapid exchange of charges back and forth until the electrode equalizes charge.

A number of effects must be considered to understand why a maximum voltage of only 110 kV was attained. A weighted average maximum energy value of an electron ejected from the daughter particles of radon gas is approximately 1.8 MeV (Firestone "*The Isotopes Project*"). Upon being ejected from the atom, the electron travels through the materials contained within the inner bulb. It collides with the isotopes and trapped helium atoms within the bulb. The collisions with the matter contained within the bulb decrease the energy of the electron. This energy loss is a function of the properties of the matter within the bulb, the distance the electron must travel, and the energy of the electron.

The electron then travels through the glass and silvered outer surface of the inner bulb. This causes the electron to lose energy in the same way it was lost to the material inside the bulb. This is also a function of the material and energy of the electron.

The electron must then travel through the partial vacuum of the inner flask, losing energy by collision with the air molecules left in the partial vacuum of the flask. This energy loss means that the energy available to climb the potential well and reach the outer flask is less than the maximum possible energy of an ejected electron.

The minimum energy an electron needs to make it to the outer flask is a function of the distance the electron travels to reach the flask and the density and makeup of the various materials through

which it must pass. Since only the electrons which have enough energy to climb the well are able to reach the outer flask, they are the only contributors to the potential.

The potential of the apparatus is also affected by γ-rays. Within the simulation, these γ-rays are created during the decomposition of lead-214 and bismuth-214. The γ-rays contain enough energy to ionize the atoms of the materials through which they pass. If a collision occurs with an electron of the outer flask, the electron gains enough energy to become unbound from the surface and, due to the potential, is drawn to the inner bulb. The electrons which are drawn back reduce the potential. This means the maximum potential of the apparatus is also a function of the energy of the photons which the isotopes produce. It should be mentioned that there is a relatively small amount of energy required to bind or dislodge the electron to the silvered surface. This value is on the order of a few eV and is insignificant when compared to the values in the simulation.

While the discharge of the apparatus due to γ-rays is relatively small, current flow along the silica rod had a much greater impact on the voltage obtained by Moseley and Fellow. They hypothesized that, due to not being thoroughly cleaned, the fused silica rod may not have had the resistance of clean silica, and a current may have traveled the length of the rod, discharging the apparatus. By running the simulation and making some assumptions about the construction of the apparatus, the value of the rod resistance was found.

Starting with 20 mCi of pure radon, which is then decayed over the four-hour period; an inner bulb of 50 mm in diameter; inner glass thickness of 0.3 mm; and a pressure inside the flask of 30.335 mTorr–enough to prevent arcing before reaching the mentioned 110 kV allowed me to try various rod resistance values.

With the rod resistance set to approximately 720 TΩ, the voltage rises to 110.2 kV. The resistivity of fused silica is 750 PΩ m (Serway 777). Assuming Figure 1 is approximately to scale, the rod's length can be estimated to be 0.37 m and, as stated in the paper, 0.8 mm in diameter. Therefore,

the clean rod's resistance should be 552 ZΩ. This would seem to confirm, just as Moseley and Fellow had thought, that the resistivity of the rod was much lower than a pure clean rod would have been.

Conclusion

Through a more modern understanding of physics and the use of computer modeling and simulation, a clearer understanding of the shortcomings and successes of Moseley's and Fellow's experiment has been discovered. With a high vacuum and smoother surface, the goal they set out to achieve was possible, but with the understanding and equipment of the time, it was not a viable means of attaining a high potential. The main effects of the voltage attained are: the energy of the electrons from the source material, the thickness of the inner bulb glass, the scattering of electrons by the produced γ-rays, the resistance of the material between the electrodes, the vacuum inside the outer flask, and the surface smoothness of the electrodes.

Computer simulations and models have given us a new way to think about the world around us, and as Sir William Bragg stated, “The important thing in science is not so much to obtain new facts as to discover new ways of thinking about them.”

Figures

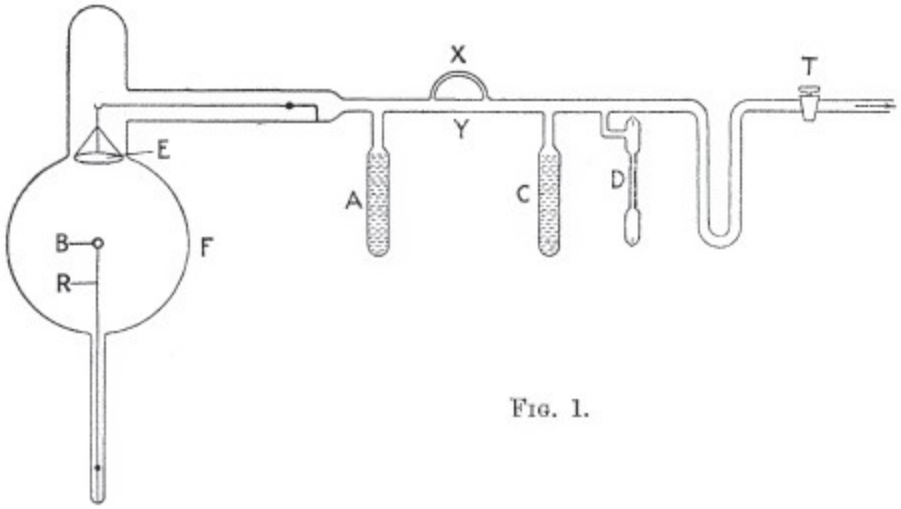

FIG. 1.

Appendix A

Capacitor

Capacitance [C.1]

$$C = \frac{Q}{\Delta V}$$

Equation **[*C.2*]** $$\Delta V = \frac{Q}{4\pi\epsilon_r}\left(\frac{1}{r_{inner}} - \frac{1}{r_{outer}}\right)$$

$$C = \frac{4\pi\epsilon_r}{\left(\frac{1}{r_{inner}} - \frac{1}{r_{outer}}\right)}$$

Voltage [C.2]

$$\Delta V = -\int \vec{E}\cdot dl$$

Equation **[*C.3*]** $$\vec{E} = \frac{Q}{4\pi\epsilon_r r^2}$$

$$\Delta V = -\frac{Q}{4\pi\epsilon_r}\int_{r_{outer}}^{r_{inner}} \frac{1}{r^2}dr$$

$$\Delta V = \frac{Q}{4\pi\epsilon_r}\left(\frac{1}{r_{inner}} - \frac{1}{r_{outer}}\right)$$

Electric Field [C.3]

$$\vec{E} = \frac{1}{4\pi\epsilon_r}\int \frac{dq}{r^2} \quad : \quad dq = \sigma R_{inner}^2 \sin\theta\, d\theta\, d\phi \quad : \quad \sigma = \frac{Q}{4\pi R_{inner}^2}$$

$$\vec{E} = \frac{Q}{4^2\pi^2\epsilon_r r^2}\int_0^{2\pi}\int_0^{\pi} \sin\theta\, d\theta\, d\phi$$

$$\vec{E} = \frac{Q}{4\pi\epsilon_r r^2}$$

Number of Ejected Electrons per Second from Gamma Rays [C.4]

$$I_s = \sigma\Phi \quad : \quad Scatters\ per\ Second = Scattering\ Cross\ Section \times Beam\ Flux$$
$$\sigma = m\mu \quad : \quad Scattering\ Cross\ Section = Mass \times Mass\ Absorption\ Coefficient$$
$$m = \rho A t \quad : \quad Mass = Density \times Area\ of\ Outer\ Sphere \times Silver\ Thickness$$
$$\Phi = n E A \quad : \quad Beam\ Flux = Number\ of\ Photons\ per\ Second \times Energy\ per\ Photon \times Area\ of\ Outer\ Sphere$$
$$I_s = \mu\rho A^2 t\, n E$$

Appendix B

Electron

Change in Electron Energy due to Moving Across an Electric Potential [E.1]

$$E_f = E_i + \Delta V$$

Time of Movement [E.2]

$$t = \frac{r}{v_r}$$

Relativistic Speed from Energy [E.3]

$$K = \frac{E_0}{\sqrt{1-u^2/c^2}} - E_0$$

$$\left(\frac{K}{E_0}\right)+1 = \frac{1}{\sqrt{1-u^2/c^2}} \quad \rightarrow \quad 1-u^2/c^2 = \frac{1}{\left[\left(\frac{K}{E_0}\right)+1\right]^2} \quad \rightarrow \quad u^2 = c^2\left(1-\frac{1}{\left[\left(\frac{K}{E_0}\right)+1\right]^2}\right)$$

$$u = c\sqrt{1-\frac{1}{\left[\left(\frac{K}{E_0}\right)+1\right]^2}}$$

Gamma Factor from Speed [E.4]

$$\gamma \equiv \frac{1}{\sqrt{1-\beta^2}}$$

$$\gamma = \frac{1}{\sqrt{1-\left(\frac{v}{c}\right)^2}}$$

Kinetic Energy from Gamma Factor [E.5]

$$p = \gamma m v \quad : \quad F = \frac{d}{dt}(\gamma m v) \quad : \quad K = \int F \cdot ds = \int \frac{d}{dt}(\gamma m v) \cdot v dt = m \int v \frac{d}{dt} dt (\gamma v)$$

$$K = m \int_0^{\gamma v} v \, d(\gamma v) \quad K = \gamma m c^2 - m c^2$$

$$K = \gamma E_0 - E_0$$

Appendix C

Unstable Isotope

Energy Distribution [U.1]

$$N = E\left(e^{-E(E_{max})}\right)\left(1-e^{E-E_{max}}\right)$$

Probability of Decay from Half-Life [U.2]

$$N = Number\,of\,Particles \quad : \quad \tau \equiv \frac{1}{p}$$

$$\frac{dN'}{dt'} = -N' p \quad \rightarrow \quad \int_0^N \frac{dN'}{N}' = -\int_0^t p \, dt' \quad \rightarrow \quad \ln(N) = -pt \quad \rightarrow \quad N = N_0 e^{-t/\tau}$$

$$N = \frac{1}{2} N_0 e^{-\lambda/\tau} \quad \rightarrow \quad \lambda = \tau \ln(2) \quad \rightarrow \quad \lambda = \frac{1}{p} \ln(2)$$

$$p = \frac{\ln(2)}{\lambda}$$

Number of Parent and Daughter Particles Left after Decay [U.3]

$$\frac{dN_1}{dt} = -p_1 N_1 \quad : \quad \frac{dN_2}{dt} = p_1 N_1 - p_2 N_2$$

$$\begin{pmatrix} \dot{N}_1 \\ \dot{N}_2 \end{pmatrix} = \begin{pmatrix} -p_1 & 0 \\ p_1 & -p_2 \end{pmatrix} \begin{pmatrix} N_1 \\ N_2 \end{pmatrix} \quad : \quad \vec{N} = \vec{A} e^{\lambda t}$$

$$\lambda \vec{A} = \begin{pmatrix} -p_1 & 0 \\ p_1 & -p_2 \end{pmatrix} \vec{A} \quad \rightarrow \quad \begin{pmatrix} -p_1 - \lambda & 0 \\ p_1 & -p_2 - \lambda \end{pmatrix} \vec{A} = 0 \quad ... \quad det \begin{pmatrix} -p_1 - \lambda & 0 \\ p_1 & -p_2 - \lambda \end{pmatrix} = 0$$

$$\lambda = -p_1, -p_2 \quad \rightarrow$$

$$\lambda = -p_1 \quad : \quad A_2 = \frac{p_1}{p_2 - p_1} A_1$$

$$\lambda = -p_2 \quad : \quad A_1 = 0$$

$$\vec{N} = A_1 \begin{pmatrix} 1 \\ \frac{p_1}{p_2 - p_1} \end{pmatrix} e^{-p_1 t} + A_2 \begin{pmatrix} 0 \\ 1 \end{pmatrix} e^{-p_2 t}$$

$$t = 0 \quad : \quad A_1 = N_{0,1} \quad : \quad A_2 = N_{0,2}$$

$$\vec{N} = N_{0,1} \begin{pmatrix} 1 \\ \frac{p_1}{p_2 - p_1} \end{pmatrix} e^{-p_1 t} + N_{0,2} \begin{pmatrix} 0 \\ 1 \end{pmatrix} e^{-p_2 t}$$

$$N_1 = N_{0,1} e^{-p_1 t} \qquad N_2 = \frac{p_1}{p_2 - p_1} N_{0,1} e^{-p_1 t} + \left(N_{0,2} - \frac{p_1}{p_2 - p_1} N_{0,1} \right) e^{-p_2 t}$$

Appendix D

Supplemental

Paschen Curve [S.1]

$$d = \frac{e^{Bpd/V_b}}{pA} \ln\left(1 + \frac{1}{v}\right) \quad \rightarrow \quad \frac{dpA}{\ln\left(1 + \frac{1}{v}\right)} = e^{Bpd/V_b} \quad \rightarrow \quad \ln\left(\frac{dpA}{\ln\left(1 + \frac{1}{v}\right)} \right) = \frac{Bpd}{V_b}$$

$$V_b = \frac{Bpd}{\ln\left(\frac{dpA}{\ln\left(1 + \frac{1}{v}\right)} \right)}$$

Bibliography

Collins, Archie Frederick. *The Wonders of Chemistry*. New York: Thomas Y. Crowell Company. 1922. Print

Firestone, Richard B. *The Isotopes Project.* Berkeley Lab. 22 Mar. 2005. Web. 17 Mar. 2013.

Moseley, H.G.J., John Harling Fellow. "The Attainment of High Potentials by the Use of Radium." *Proceedings of the Royal Society of London. Series A.* 88.605 (1913): 471-476. Print.

Serway, Raymond A., and John W. Jewett, Jr. *Physics for Scientists and Engineers*. Belmont: Brooks/Cole. 2010. Print

Wadhwa, C.L. *High Voltage Engineering.* New Delhi. New Age International. 2007. Print.